

# Dust transport model validation using satellite- and ground-based methods in the southwestern United States

Anna-Britt Mahler<sup>a</sup>, Kurt Thome<sup>a</sup>, Dazhong Yin<sup>b</sup>, William A. Sprigg<sup>b</sup>

<sup>a</sup>College of Optical Sciences, University of Arizona, 1630 E University Blvd, Tucson, AZ;

<sup>b</sup>Department of Atmospheric Sciences, University of Arizona, 1118 E 4th Street, Tucson, AZ

## ABSTRACT

Dust is known to aggravate respiratory diseases. This is an issue in the desert southwestern United States, where windblown dust events are common. The Public Health Applications in Remote Sensing (PHAiRS) project aims to address this problem by using remote-sensing products to assist in public health decision support. As part of PHAiRS, a model for simulating desert dust cycles, the Dust Regional Atmospheric Modeling (DREAM) system is employed to forecast dust events in the southwestern US. Thus far, DREAM has been validated in the southwestern US only in the lower part of the atmosphere by comparison with measurement and analysis products from surface synoptic, surface Meteorological Aerodrome Report (METAR), and upper-air radiosonde. This study examines the validity of the DREAM algorithm dust load prediction in the desert southwestern United States by comparison with satellite-based MODIS level 2 and MODIS Deep Blue aerosol products, and ground-based observations from the AERONET network of sunphotometers. Results indicate that there are difficulties obtaining MODIS L2 aerosol optical thickness (AOT) data in the desert southwest due to low AOT algorithm performance over areas with high surface reflectances. MODIS Deep Blue aerosol products show improvement, but the temporal and vertical resolution of MODIS data limit its utility for DREAM evaluation. AERONET AOT data show low correlation to DREAM dust load predictions. The potential contribution of space- or ground-based lidar to the PHAiRS project is also examined.

**Keywords:** Public health warning system, DREAM, dust transport, model evaluation, aerosol optical thickness, MODIS, AERONET, lidar.

## 1. INTRODUCTION

### 1.1. Importance of studying aerosol transport

Respiratory diseases, asthma, allergies and eye infections caused or aggravated by dust threaten public health in the desert southwestern United States, where windblown dust events are common. For example, valley fever (coccidioidomycosis) is caused by a fungus that produces spores that can be inhaled when airborne.<sup>1</sup> Additionally, loss of visibility due to dust storms causes numerous vehicle accidents in the southwestern US, some of which are fatal. Dust also plays an important role in weather<sup>2</sup> and in climate forcing throughout the entire year by scattering solar radiation back at visible wavelengths, absorbing solar radiation at infrared wavelengths, and by shading the earth's surface. Airborne particles provide a nucleus for cloud condensation, affecting cloud formation and changing the hydrological cycle.<sup>3</sup> Aerosol scattering and absorption is also an area of great interest to the remote sensing community. For example, radiative transfer codes such as MODTRAN depend upon accurate aerosol distribution models to correctly model the transmission and absorption of light as it passes through the atmosphere.<sup>4</sup>

Substantial impacts of dust on climate and environment such as those mentioned above highlight the need for a solid understanding of atmospheric dust cycles. Because aerosol content is very dynamic, an estimate for a given time or location cannot be extended over long time periods or large areas without significant error. Thus, accurately modeling aerosol distribution and transport is valuable in an immediate sense for public health and safety and in order to provide better estimates for climate forcing and remote sensing purposes.

---

Further author information: Send correspondence to A.M. E-mail: mahler@email.arizona.edu

## 1.2. Dust and aerosol Characteristics

The dominant aerosol in the lower atmosphere is windblown dust composed primarily of clay and sea salt mineral particles, with a small amount of organic matter.<sup>5</sup> The large particle size of most of this dust usually results in high settling rates, but under some conditions these dust particles can spread far from their source and remain in the atmosphere for long periods.<sup>5</sup> The primary components of windblown surface dust are quartz, calcite, oxides of iron and clay minerals (montmorillonite and illite). Sizes are 1-10  $\mu\text{m}$  and this dust accounts for approximately 30% of atmospheric aerosols globally.<sup>5</sup>

Typical parameters used to describe aerosols are the size distribution, the single scatter albedo, the phase function, the extinction coefficient, and aerosol optical thickness. Aerosol size distribution describes the number of particles present at a given radius. Single scatter albedo ( $\omega_0$ ) quantifies the amount of energy scattered by a particle. The aerosol scattering phase function ( $P_a(\theta)$ ) describes the angular distribution of this scattered energy.<sup>6</sup> The extinction coefficient ( $\sigma_e$ ) is the fractional loss in beam intensity per meter due to scattering and absorption.<sup>7</sup> Aerosol optical thickness, or AOT ( $\delta$ ), describes the degree to which aerosols prevent the transmission of light. Vertical AOT is defined as the aerosol extinction coefficient integrated over the atmospheric column. Type and concentration of aerosols as well as the wavelength of radiation that is interacting with the aerosols are required to characterize aerosol absorption.<sup>6</sup>

## 1.3. PHAiRS project

Public health hazard concerns are being addressed by the Public Health Applications in Remote Sensing (PHAiRS) project, which is using NASA remote sensing products to enhance an existing public health decision support system.<sup>8</sup> The PHAiRS project has adapted an existing model for simulating desert dust cycles (developed by Nickovic, et. al.<sup>9</sup>) to the southwestern US in order to forecast dust events and concentrations. This model, the Dust Regional Atmospheric Model (DREAM), provides essential information that is to be integrated into a system that will issue timely, accurate, site-specific early warning of desert dust pollution episodes. Appropriate actions can then be taken to avoid unnecessary exposure to dust pollution.<sup>10</sup>

The purpose of this work is to determine the most appropriate data sets with which to validate the output from DREAM in the desert southwestern US using remote sensing approaches. The evaluation investigates both ground- and satellite-based approaches. A brief description of the DREAM model follows as well as an overview of the validation methods.

### 1.3.1. DREAM

DREAM is an eulerian model and obtains input from two main source modules. The first is the dust concentration module. This module requires topography, vegetation cover and soil types. The second is the atmospheric modeling module, which requires inputs such as humidity, and wind patterns.<sup>8</sup>

The DREAM model calculates various parameters at equally-spaced points in the focus area grid on an hourly basis. Meteorological outputs include mean sea level pressure fields, 500 hPa geopotential height fields, temperature fields and height profiles, wind speed height profiles, specific humidity height profiles, and wind direction height profiles.<sup>10</sup> Dust field outputs include both PM2.5 and PM10 near ground layer dust concentrations. PM2.5 and PM10 are the masses of those particles with diameters less than 2.5  $\mu\text{m}$  and 10  $\mu\text{m}$ , respectively. These particles are small enough to be inhaled and penetrate below the larynx.<sup>7</sup>

### 1.3.2. DREAM model validation efforts

In general, the model has already demonstrated the ability to reproduce major features of atmospheric dust cycle over the Mediterranean and Asia, as compared with lidar, SeaWiFS and AERONET measurements.<sup>9</sup> The model has since been adapted to the southwestern US, and as mentioned, this study seeks to validate the model in this region. To this end, the model was applied to a dust storm case in December, 2003, and results of that study indicate that the model predicted meteorological fields reasonably well.<sup>10</sup> Specifically, the modeled 500 hPa geopotential height and temperature fields are in agreement with the measured geopotential height and temperature fields. Predicted vertical profiles of wind, temperature, and humidity closely resemble the observed profiles. Satellite images of the dust event show a visual outline of the dust clouds, and the modeled spatial distribution was comparable to both the satellite visual outline and to measured reduced visibility patterns.

The model-predicted and observed PM<sub>2.5</sub> peak hours matched reasonably well with those measured using filter techniques in the lower 3 meters of the atmosphere. The time-varying trends of daily and hourly PM<sub>2.5</sub> and PM<sub>10</sub> concentrations at most of the measurement sites were similar, though sometimes the modeled and measured concentrations had differences of one order of magnitude.<sup>10</sup>

## 2. DREAM EVALUATED WITH MODIS L2 AEROSOL DATA

The Moderate Resolution Imaging Spectroradiometer (MODIS) is on both the Aqua and the Terra platforms. MODIS Terra has a descending morning crossing time and MODIS Aqua has an ascending afternoon crossing time. MODIS is a scanning system with 36 spectral bands, spanning the wavelengths from 0.4 to 14.4  $\mu\text{m}$ . A  $\pm 55$  degree scanning pattern at the the Terra and Aqua orbits of 705 km allows a 2330 km swath width and global coverage every two days.<sup>12</sup> MODIS was chosen for this study due to its high frequency of overpass, large area coverage and readily available, validated AOT product.

### 2.1. Method

Candidate dust events for comparing output of the DREAM model in the southwestern United States to MODIS L2 aerosol products were located in two ways. First, the NASA Earth Observatory archive of natural hazard smoke and dust events contained eight dust events in the desert southwest that are clearly observed in the associated visible imagery. MODIS L2 AOT and calibrated radiance data were investigated for each of these events. Second, a search of Lexis Nexis, a university library database of newspaper articles, revealed 38 local and regional dust storms over the last four years in the southwestern US, most of which caused fatal car accidents on major highways. MODIS L2 AOT data were investigated for the 26 events occurring over desert terrain.

### 2.2. Description of the MODIS L2 AOT algorithm over land

The MODIS aerosol retrieval algorithm masks all pixels found to contain any clouds, snow/ice or water. Pixels passing low reflectance requirements in the 2.13  $\mu\text{m}$  band are used to estimate the expected reflectance in the 0.66  $\mu\text{m}$  band using an empirical relationship.<sup>13</sup> The expected reflectance in the 0.66  $\mu\text{m}$  band is compared with the actual value, and the difference between the two values is attributed to aerosol scattering. Aerosol type is then determined using information on the global aerosol distribution and the ratio between the aerosol path radiance in the red and blue channels.<sup>13</sup> The aerosol type information guides the selection of an appropriate aerosol model that describes the aerosol size distribution, refractive index, single scattering albedo and effect of nonsphericity on the phase function. Radiative transfer look-up tables are computed from the measured radiances and the parameters from the aerosol model. Thus, via an aerosol type determination, and aerosol model determination and a radiative transfer lookup table, the measured radiance from the satellite is converted into AOT. Pixels that do not pass the initial reflectance requirements will not return an AOT value.<sup>13</sup> The MODIS L2 AOT product is provided in 10 km by 10 km pixels.

### 2.3. Results

The expected result in the vicinity of a reported dust event was that the AOT product would show well-defined areas of elevated dust concentration. With a few exceptions, the expected elevated values of AOT in the region of the dust events is not observed in the MODIS L2 AOT product. In general, for the desert southwestern US, pixels returning AOT values seem to be interspersed with many pixels of no data.

Three image pairs are shown here illustrating the above using the results of the AOT algorithm at 550 nm. Dark grays indicate low AOTs, light grays indicate high AOTs, and black pixels indicate no data. Typically, the maximum value for AOT in a given data set varies between 1 and 2.3, and the minimum value is zero. The 15 December 2003 dust event shown in figure 1 was identified from the NASA Earth Observatory archive, and occurred over both Texas and New Mexico. Dust events are observed both in southeastern New Mexico and northern Mexico and in north central Texas. Neither event is observed in the AOT product (right panel). The 23 July 2003 event shown in figure 2 was identified from the NASA Earth Observatory archives, and occurred near Great Salt Lake in Utah. The smoke events can be identified in the Terra MODIS L2 AOT data but no AOT data are retrieved over the dust event (right panel). On 15 April 2003, strong winds blew from northern Mexico into western Texas and southern New Mexico. Figure 3 shows dust plumes arching from the source region into

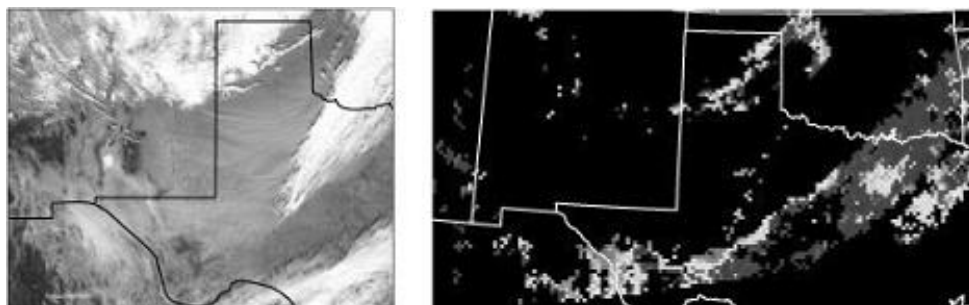


**Figure 1.** 15 December 2003 dust event over Texas and New Mexico. Dust observed in the Aqua MODIS true color composite (left panel). Corresponding dust pixels not observed in the MODIS L2 AOT product (right panel).

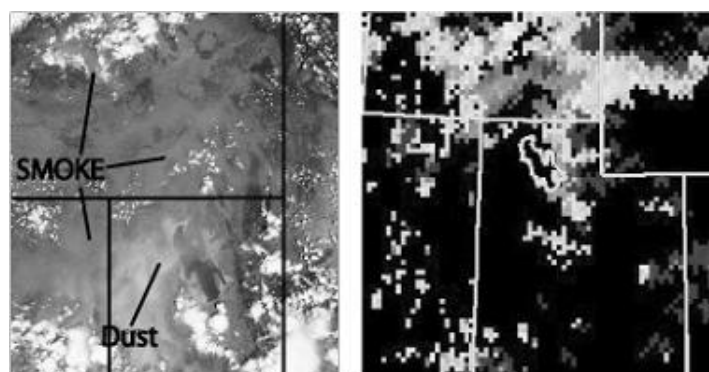


**Figure 2.** 23 July 2003 dust event near Great Salt Lake, UT. The smoke events can be identified in the Terra MODIS L2 AOT data but the dust event cannot (right panel).

TX and NM in the Aqua MODIS image (left panel). However, no Aqua MODIS L2 AOT data are retrieved near the dust storm (right panel). This dust event is similar to the 15 December, 2003 dust event in its location. Additionally, both dust events were caused by strong winds. Elevated AOT concentrations are observed to the southeast of the dust event, in the same area where clouds are seen in the image. The image and AOT results are from the same Aqua MODIS overpass, so it is unknown why the cloud mask allowed AOT retrieval in pixels clearly filled by clouds.

Additional dust events were located by searching a university database of newspaper articles. MODIS L2 AOT data were obtained for the reported date of the dust event. These data sets are difficult to interpret because the time of the dust storm in each location was not reported, so it is unknown what the conditions were at the time of overpass. In the majority of cases, no AOT data are obtained near the reported location of the dust storm.

## 2.4. Discussion

There are many possible reasons for the lack of AOT data coincident with dust events. First, for the Lexis Nexis dust events, the time of the event was not reported, so the overpass time may not be concurrent with the dust event. Second, as explained previously, surface reflectance thresholds prevent the algorithm from retrieving AOT. The aerosol optical thickness algorithm for land is designed to work best over dark, vegetated areas. Most of the southwestern United States is not accurately described as dark or vegetated, which may explain why the algorithm is not returning spatially continuous data, but rather patches of data. An additional complicating factor is that dust events tend to raise reflectance. In figures 1 through 3, the dust events are bright compared to the background. If dust has a reflectance higher than 0.4, such as the dust plume seen in figure 1 in northern Mexico, those pixels with elevated dust concentration will not pass the required reflectance threshold and thus

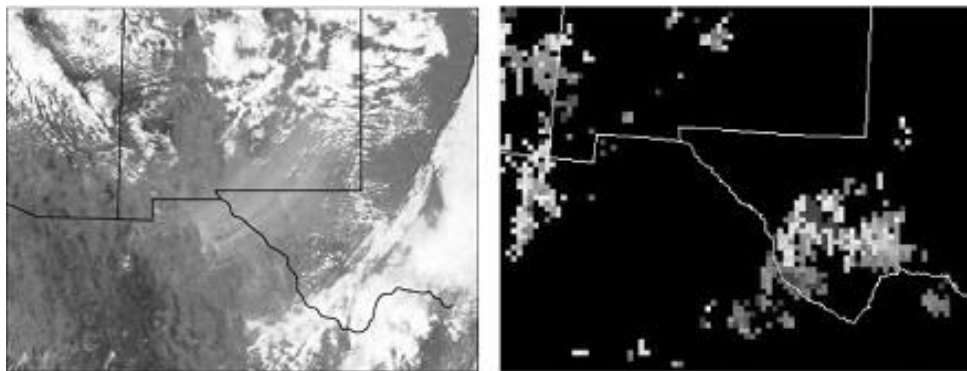


**Figure 3.** 15 April 2003 dust storm in Texas and New Mexico caused by strong winds from northern Mexico. Dust plumes are visible from the source region into TX and NM in the Aqua MODIS true color image (left panel), but no Aqua MODIS L2 AOT data are retrieved over the area corresponding to the dust plumes (right panel).

will not return an AOT value. Third, many dust storms in the desert southwestern US are caused by high winds which are accompanied by clouds,<sup>11</sup> as seen in figures 1 and 3. The MODIS L2 AOT algorithm screens cloudy pixels, so if a dust storm is occurring during cloudy conditions, the AOTs for those pixels may not be retrieved.<sup>13</sup>

In summary, MODIS AOT values cannot be reliably retrieved over dust events in the desert southwestern US using the current algorithm due to algorithm retrieval limitations over highly-reflective surfaces. Thus, comparison between DREAM and MODIS L2 AOT data will not be sufficient for evaluating the DREAM model in this region. An improved algorithm is needed to address the problem AOT retrieval over bright surfaces. The following section discusses the new MODIS Deep Blue AOT algorithm and its contribution to DREAM model evaluation.

### 3. DREAM EVALUATED WITH MODIS DEEP BLUE AEROSOL DATA

#### 3.1. Deep Blue Algorithm

An approach for AOT retrieval over arid, semiarid and urban areas, called Deep Blue, has been developed<sup>14</sup> and is used in this study. Deep Blue takes advantage of the fact that desert surfaces typically have lower reflectances at short wavelengths. Before the aerosol retrieval processing begins, pixels with clouds, snow and ice are screened. An assumed surface reflectance for each pixel is determined for the 412 nm, 490 nm and 670 nm channels from a database of reflectance values based upon geographic location and scene geometry. The at-sensor radiances in these channels are then compared to radiances from a lookup table based upon solar, satellite, and azimuth angles, the assumed surface reflectance, a range of aerosol optical thickness, and a range of single scatter albedo. A maximum likelihood method determines the aerosol optical thickness and single-scattering albedo needed to give predicted at-sensor radiances that matches both the magnitude and spectral characteristics of the measured radiances.<sup>14</sup> AOT retrieved by the MODIS Deep Blue algorithm has been compared to ground-based AERONET AOT data. Retrievals from the two instruments are consistently within 20%.<sup>15</sup> Additionally, the calibration and signal-to-noise ratio of the MODIS sensor are sufficiently accurate to minimize sensor effects on MODIS AOT retrievals.<sup>16</sup>

#### 3.2. Method

The utility of the Deep Blue algorithm for DREAM validation is evaluated in this section. From the geometrically registered DREAM and MODIS AOT images, the DREAM AOT for a given location is compared against the corresponding AOT from the MODIS Deep Blue data and a correlation coefficient,  $r^2$ , is calculated.



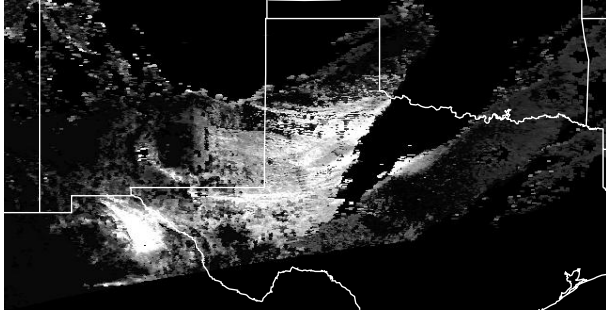


**Figure 4.** MODIS Aqua Deep Blue AOT data on a 0.025 by 0.025 degree grid for 15 Dec 03, 2000 GMT dust event over western Texas. Lighter grays indicate higher AOTs. Black indicates no data.

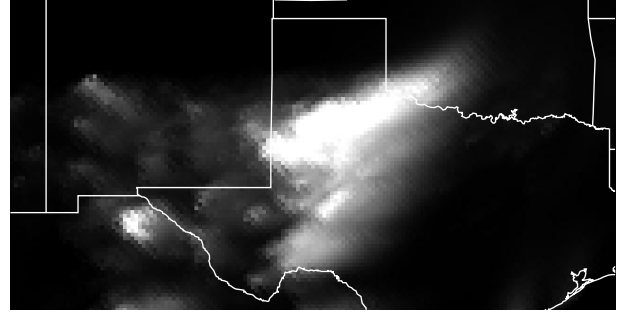


**Figure 5.** DREAM dust load ( $\text{g/m}^2$ ) data on a 0.025 by 0.025 degree grid for 15 Dec 03, 2000 GMT dust event over western Texas. Lighter grays indicate higher AOTs. Black indicates no data.

**Table 1.** The four DREAM dust categories and their particle properties<sup>10</sup>

Dust bin	Particle size bin ( $\mu\text{m}$ )	Typical radius ( $\mu\text{m}$ )	Density ( $\text{kg/m}^3$ )
1	0-3.4	0.73	2500
2	3.4-12	6.10	2650
3	12-28	18.00	2650
4	28-38	38.00	2650

### 3.2.1. Processing of MODIS AOT data

MODIS Aqua Deep Blue AOT data from 15 December, 2003, 2000 GMT were provided in a radiometrically and geometrically corrected format on a 0.025 by 0.025 degree grid, as seen in figure 4. Lighter grays indicate higher AOTs, darker grays indicate lower AOTs, and black indicates zero values. The maximum value is 4 and the minimum value is zero. The data provided did not differentiate pixels of no data due to cloud-screening or the data extent from pixels with AOTs of zero, so all pixels with having a value of zero were excluded from this analysis. An example of zeros due to cloud-screened pixels is the two lobes of black pixels on the top of the image. Zeros due to the edge of the MODIS data are seen on the lower part of the image. Dust plumes are evidenced by the westward-sweeping features in the center of the image.

### 3.2.2. Processing of DREAM dust load data

DREAM calculates dust load, the mass per unit volume of the dust aerosols integrated over the atmospheric column, in each of four size bins, each of which has a typical particle radius, particle density and associated soil component. During the evolution of the dust storm, the number of particles in each bin is changing for a given point in the atmosphere. The vertical sum of these binned dust loads gives the total dust load.<sup>10</sup> The DREAM output used in this comparison is the map of dust load ( $\text{g/m}^2$ ), converted into AOT. This data set, also from 15 December, 2003, 2000 GMT, was provided in a georeferenced format on a 0.1 by 0.1 degree grid. Each pixel was segmented into 16 pixels with identical values to match the 0.025 by 0.025 degree grid of the MODIS Deep Blue data. An example of DREAM dust load data on this 0.025 by 0.025 degree grid is shown in figure 5. Again, lighter grays indicate higher dust loading, darker grays indicate lower dust loading, and black indicates zero values. The maximum value is  $4.79 (\text{g/m}^2)$  and the minimum value is zero. There is a high concentration of dust predicted in north central Texas, where the MODIS data shows the dust event occurring.

In order to convert DREAM dust load values into AOTs, the size distribution of the aerosols is assumed to follow the Junge distribution, which takes the form:<sup>17</sup>

$$\frac{dn(r)}{dr} = C(z)r^{-\nu+1}$$

where  $r$  is particle radius,  $dr$  is the change in radius in a given bin,  $C(z)$  is a scaling factor directly proportional to the aerosol concentration,  $z$  is altitude,  $\nu$  represents a shaping constant which normally takes a value between 2 and 4, and  $dn(r)$  is the number of particles of a given radius per area, calculated as

$$dn(r) = \frac{M}{V\rho}$$

where  $M$  is dust load,  $V$  is particle volume and  $\rho$  is particle density. Typical particle volumes and densities are found in table 1. The value of  $C(z)$  for each bin is needed to find the constant  $k$ :<sup>17</sup>

$$k = \pi(2\pi)^{\nu-2} \int_0^\infty C(z)dz \int_{x_1}^{x_2} \frac{Q_e(x, \lambda)dx}{x^{\nu-1}}$$

where the extinction efficiency,  $Q_e$  is expressed in terms of the size parameter  $x = 2\pi r/\lambda$ . The value of  $x$  is calculated for each bin using the typical particle radii given in table 1, and these values are used to calculate  $Q_e$ . The coefficient  $k$  is needed for each bin to calculate AOT:

$$\delta(\lambda) = k\lambda^{-\nu+2}$$

When all of the above equations are combined and simplified in summation form, the final result is the following equation for conversion from dust load into AOT,

$$\delta(\lambda) = \sum_{i=1}^4 \frac{3}{4r_i\rho_i} M_i Q_e(x, \lambda)_i$$

where  $i$  is the bin number index.

### 3.3. Results

The scatterplot of MODIS Deep Blue AOT values vs. corresponding DREAM AOT values for the 15 December 2003 data is shown in figure 6. The correlation coefficient for these data is  $r = 0.59$  ( $r^2 = 0.35$ ). The scatterplot of MODIS L2 AOT values vs. corresponding DREAM AOT values for the 15 December 2003 data is shown in figure 7 and has a correlation coefficient of  $r = 0.20$  ( $r^2 = 0.04$ ).

### 3.4. Discussion

The two scatterplots show different maximum values for the same DREAM data set. This is because all pixels having a value of zero in the MODIS data were excluded from the comparison, as explained in section 3.2.1. As mentioned in section 1.2, vertical AOT is defined as the aerosol extinction coefficient integrated over the atmospheric column, where the extinction coefficient is the fractional loss in beam intensity per meter due to scattering and absorption.<sup>7</sup> The MODIS Deep Blue AOT product is measuring the extinction due to all aerosols, but the DREAM AOT only takes dust aerosols into account. This difference may help to account for the fact that DREAM AOT predictions are low by approximately a factor of two as compared to MODIS AOT measurements. A correlation coefficient of 0.59 ( $r^2 = 0.35$ ) shows a positive relationship between the measured and predicted AOT values, but is not considered a strong correlation. However, given that observed data are compared to modeled data in this work, these results are encouraging.

The deep blue algorithm shows better correlation to DREAM data than the MODIS L2 data. The deep blue algorithm is clearly an improvement over the L2 algorithm for AOT retrieval in the desert southwestern US for the purpose of evaluating the DREAM model. However, despite encouraging results, lack of temporal and vertical resolution and the nature of dust storm evolution in this region limit the utility of MODIS deep blue aerosol data for DREAM model evaluation. Additional techniques of aerosol measurement will be necessary to adequately evaluate the DREAM model in the desert southwestern US. The following section evaluates DREAM by comparison to ground-based AOT measurements.

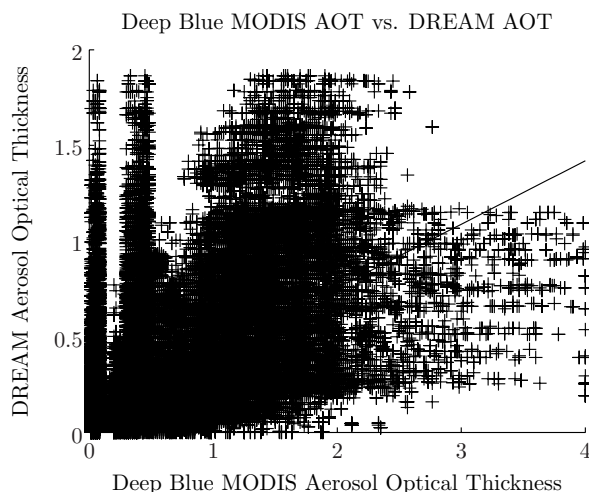


**Figure 6.** Scatterplot of MODIS Deep Blue AOT data vs. DREAM AOT data for 15 Dec 03, 2000 UTC.  $r = 0.59$ ,  $r^2 = 0.35$ .

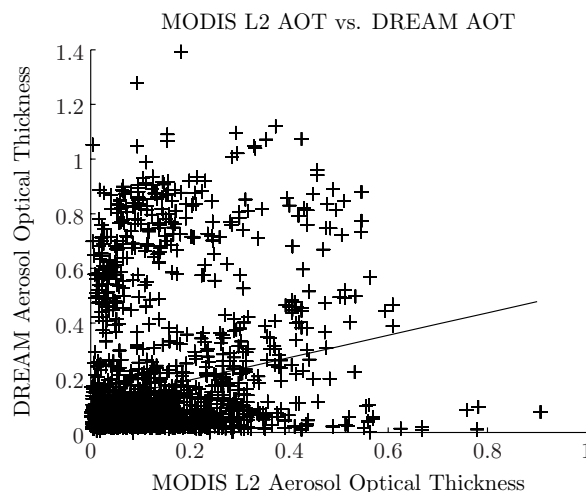


**Figure 7.** Scatterplot of MODIS L2 AOT data vs. DREAM AOT data for 15 Dec 03, 2000 UTC.  $r = 0.20$ ,  $r^2 = 0.04$ .

## 4. DREAM EVALUATED WITH AERONET DATA

### 4.1. AERONET

The AERONET (AErosol RObotic Network) program is an inclusive federation of ground-based remote sensing CIMEL sunphotometers. The program goal is to assess aerosol optical properties and validate satellite retrievals of aerosol optical properties.<sup>19</sup> The network imposes standardization of instruments, calibration, and processing. AERONET provides well-calibrated aerosol data to which DREAM predictions can be compared. The CIMEL Electronique 318A spectral radiometer is a solar-powered, weather-hardy, robotically-pointed sun and sky spectral radiometer with a 1.2 degree field of view.<sup>18</sup> The total spectral optical depth is the sum of the Rayleigh and aerosol optical depths after correction for gaseous absorption.<sup>18</sup> The CIMEL sunphotometers use Beer's Law to retrieve spectral direct sun AOT and Langley plots, and spectral sky radiance allows retrieval of scattering AOT.<sup>18</sup> The total uncertainty in AOT from a newly calibrated field instrument under cloud-free conditions is usually less than  $\pm 0.01$  for wavelengths greater than  $0.44 \mu\text{m}$ , and less than  $\pm 0.02$  for shorter wavelengths.<sup>18</sup> These uncertainties arise from instrumental, calibrational, atmospheric and methodological factors that influence the precision and accuracy of optical depth determination.<sup>18</sup>

### 4.2. Method and results

Within the area of the December 2003 dust event, there are 13 AERONET sunphotometer sites, two of which were active during the December 2003 dust event. The first, in Tucson, AZ, is operated by the Remote Sensing Group at the University of Arizona. The second, in Los Alamos, NM, is operated by Brad Henderson of Los Alamos National Laboratory. The DREAM algorithm predicted dust load values hourly for the days between December 8-10 and December 14-17, 2003. DREAM dust load values were converted to AOTs at  $0.5 \mu\text{m}$  using the same method explained in section 3.2.2. Unscreened level 1 AERONET AOT data at  $0.5 \mu\text{m}$ , taken with irregular time increments, were downloaded for the days of the DREAM model run.

Scatterplots are shown of AERONET level 1.0 unscreened AOT vs. DREAM AOT for Tucson, Los Alamos, and the combined data. Although level 1 data may contain cloud contamination, level 1.0 data were used instead of the cloud-screened level 1.5 data because the dust events may have been screened out of the cloud-screened data. Each AERONET data point closest to the top of the hour was chosen for comparison to the hourly DREAM predictions. These data are generally no greater than 10 minutes apart. AERONET AOT vs. DREAM AOT for Tucson, shown in figure 8, has  $r = 0.16$  and  $r^2 = 0.02$ , which indicates very little correlation. AERONET AOT vs. DREAM AOT for Los Alamos, shown in figure 9, has  $r = 0.62$  and  $r^2 = 0.39$ , which indicates a



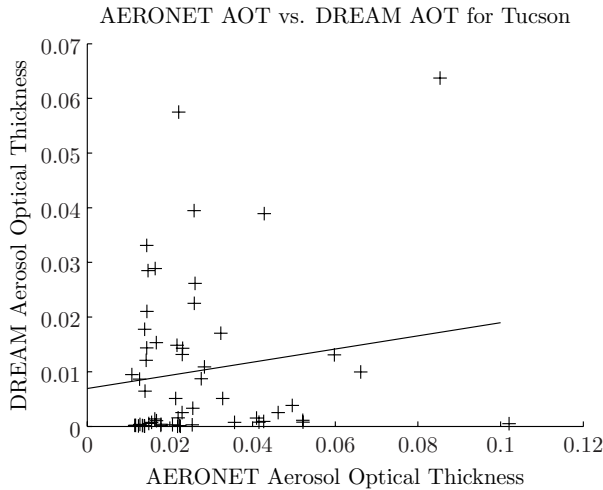


**Figure 8.** AERONET AOT vs. DREAM AOT for Tucson ( $r = 0.16$  and  $r^2 = 0.02$ ).

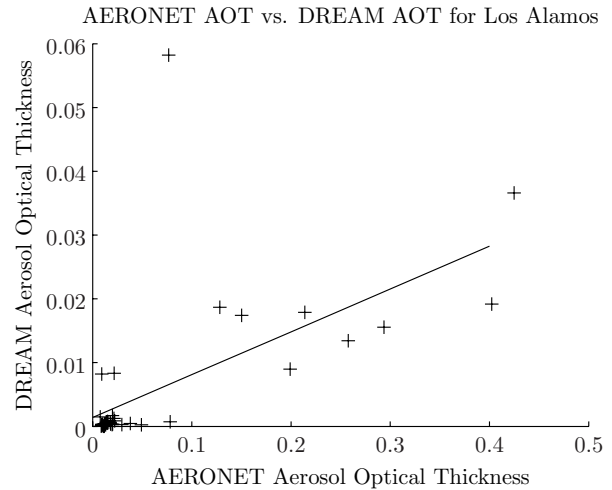


**Figure 9.** AERONET AOT vs. DREAM AOT for Los Alamos ( $r = 0.62$  and  $r^2 = 0.39$ ).

positive correlation but not a strong correlation. In summary, AERONET and DREAM AOT data for the days surrounding the December 15 dust event are not strongly correlated.

### 4.3. Discussion

AERONET retrieval accuracy is limited most by low AOT situations for all aerosol types, where high relative errors may occur in the direct radiation measurements of aerosol optical depth.<sup>19</sup> Many of the AOT values used in this analysis are low, and the comparison to DREAM AOT may be affected by this additional uncertainty. Additionally, there may not be much dust in the atmosphere to observe. AOT values greater than 0.2 may include a significant amount of dust aerosols,<sup>11</sup> and AOT values greater than 0.5 are considered heavy dust conditions.<sup>14</sup> All but one of the level 1.0 AERONET AOT values compared here are less than 0.1 in Tucson and less than 0.45 in Los Alamos. However, the high values (0.2-0.4) measured in Los Alamos may be due to cloud contamination instead of dust aerosols. Thus, the measured AOT values are not likely to include a significant contribution from dust aerosols in either location. Measured total aerosols and predicted dust aerosols may not agree unless high dust loading occurs.

This analysis shows that the desert southwestern US is a difficult region in which to measure aerosol properties, even with a well-validated, ground-based method such as AERONET. In order to adequately characterize the strengths and shortcomings of DREAM, additional techniques of aerosol measurement will be necessary. The following section details how lidar data might contribute to DREAM evaluation if an instrument were available for this purpose.

## 5. DREAM EVALUATION USING LIDAR DATA

DREAM predictions at various altitudes have not yet been evaluated in the southwestern US. A ground- or satellite-based lidar (LIght Detection And Ranging) system would exactly suit this task, because lidars are able to assess dust structure and optical properties with high vertical resolution.<sup>20</sup> Lidar data can be collected during both day and night, so the temporal coverage can be more complete than AERONET data. However, like AERONET, a lidar system is located at a single point in latitude and longitude, so regional measurements require multiple lidar systems. If a lidar system could be obtained for DREAM validation in the southwestern US, a qualitative and quantitative comparison of aerosol profiles could be obtained.

## 5.1. Ground-based lidar

An atmospheric lidar sends out a beam or a pulse of light, which travels through the atmosphere, encountering aerosols and molecules that scatter the light. A small fraction of that light is then backscattered into the detector. A micro-pulse lidar (MPL) system with a Nd:YLF (neodymium: yttrium lithium fluoride) laser with a fundamental wavelength of 1046 nm would be good choice for this application because these lasers have been shown to be rugged and are relatively common. The wavelength can be converted to 532 nm for use in the lidar if passed through a doubling crystal.<sup>21</sup>

The lidar equation can be written as<sup>22</sup>

$$\beta_a(x-1) = \frac{P_r(x-1)\Psi(x-1, x)}{\frac{P_r(x)}{\beta_a(x)+\beta_m(x)} + S_a[P_r(x) + P_r(x-1)\Psi(x-1, x)]\Delta z} - \beta_m(x-1)$$

where  $P_r(x)$  is the range-corrected lidar signal at altitude  $x$ ,  $\beta(z)$  is the backscatter coefficient, and  $S(z)$  is the extinction-to-backscatter ratio, given by  $S(z) = \frac{\sigma(z)}{\beta(z)}$  where  $\sigma(z)$  is the extinction coefficient.  $m$  and  $a$  subscripts indicate contributions from molecular and aerosol scattering, respectively.<sup>21</sup>

$$\Psi(x-1, x) = \exp [(S_a - S_m) (\beta_m(x-1) + \beta_m(x)) \Delta z]$$

and where  $x-1$  is the altitude bin just below  $x$  and  $\Delta z$  is the lidar range interval. Molecular atmosphere scattering properties,  $\beta_m$  and  $\sigma_m$ , can be determined from meteorological data or approximated from appropriate standard atmospheres.<sup>22</sup> In order to invert this equation for aerosol profiles, one solution would be to assume that  $S_a$  and  $\beta_a$  are constant with range.<sup>22</sup> This means that the size distribution and composition of the aerosol scatterers are not changing within layers, though they can be different in different layers. A maximum altitude,  $z_{max}$ , must first be chosen where no aerosols appear to be present. At this height,  $\beta_a(z)$  is set equal to zero.<sup>21</sup> Second,  $\beta_a(z)$  must be calculated one altitude step below  $z_{max}$  by solving the lidar equation for  $\beta_a(x = z_{max}) = 0$ .  $S_a$  is set equal to 1 and  $\beta_a(x-1)$  is calculated. This process is repeated down through the atmosphere, with  $R_a$  equal to 1 and  $\beta_a(x+1)$  taken from the previous step, until  $\beta_a$  is calculated in the lowest altitude bin.<sup>21</sup> Third, an improved estimate of  $S_a$ ,  $S_{a,new}$ , is obtained using the  $\beta_a(z)$  profile calculated previously via the equation

$$S_{a,new} = \frac{\int_{z_L}^{z_m} \beta_a(z') dz'}{\delta_a}$$

where  $\delta_a$ , the integrated quantity of  $\sigma_a$  over the atmospheric column, is an AOT measurement taken from a sunphotometer at the time of the lidar measurement.<sup>21</sup> The  $\beta_a$  profile is recalculated using  $\beta_a(x = z_{max}) = 0$  and  $S_{a,new}$ . This iterative process continues until  $S_a$  and  $S_{a,new}$  agree to within 0.5 %.<sup>21</sup> The final  $\beta_a(z)$  profile and  $S_a$  value are then used to calculate the extinction coefficient profile,  $\sigma_a(z)$ . An AOT profile,  $\delta_a(z)$ , is calculated by numerically integrating  $\sigma_a(z)$  values in each bin.

Lidar AOTs measured at 532 nm could be compared with DREAM-modeled AOTs after conversion from dust load, as shown in section 3.2.2. Also, the daily evolution of the vertical dust structure observed by the lidar can be qualitatively and quantitatively compared to the dust structure predicted by DREAM.

One drawback to this method is that it relies upon sunphotometer data, so lidar measurements would not be independent of sunphotometer measurements. Also, significant uncertainties may result due to the assumption of a constant extinction-to-backscatter ratio value.<sup>21</sup> For instance, if there is a smoke layer above a dust layer, the composition of these layers will not be constant, so  $S(z)$  will not be constant and the method will not return accurate results. In order to avoid making this assumption, other methods such as dual wavelength or raman lidar could be used.<sup>21</sup>

## 5.2. DREAM evaluation using satellite-based lidar

The Cloud-Aerosol Lidar and Infrared Pathfinder Satellite Observation (CALIPSO) satellite was recently launched with the cloud profiling radar system on the CloudSat satellite. CALIPSO will combine an active lidar instrument with passive infrared and visible imagers to probe the vertical structure and properties of thin clouds and

aerosols over the globe. The expected lifetime of the system is 3 years.<sup>23</sup> Though CALIPSO has only a 100 m footprint on the ground, its advantage over passive imaging is the ability to operate over bright and heterogeneous land surfaces and at night.<sup>23</sup>

When data become available for public use, aerosol profile products from CALIPSO can be compared to modeled dust profiles from DREAM to determine how well the model is performing vertically. Additionally, CALIPSO AOT values can be compared to modeled DREAM output after converting column-integrated DREAM size distribution information into AOT, as shown in section 3.2.2. In these ways, analysis of the spatial extent of dust clouds may be feasible. Thus, CALIPSO will soon be an additional source of data for DREAM evaluation.

### 5.3. Discussion

Ground-based lidar offers high temporal and vertical resolution, and satellite-based lidar offers high vertical resolution. Unfortunately, the long (16 day) revisit time and the high uncertainties associated with the satellite-based lidar will limit the utility of the data for DREAM evaluation in the desert southwestern US. Though lidar offers the unique contribution of vertical resolution to the DREAM evaluation effort, additional methods of aerosol measurement are required to adequately evaluate the DREAM model in the desert southwestern US.

## 6. CONCLUSIONS

DREAM has been validated in the Mediterranean using lidar, sunphotometer, satellite and synoptic charts of geopotential height and pressure.<sup>20</sup> For the 15 December, 2003 dust event in Texas and New Mexico, DREAM atmospheric parameters were previously validated, but only in the lower 3 meters of the atmosphere.<sup>10</sup> This work compares AOT values derived from the DREAM dust load output to AOT values from MODIS L2, MODIS Deep Blue, and AERONET measurements for this same 15 December, 2003 dust event. The potential contribution of ground- and satellite-based lidar data to the DREAM validation effort is also discussed.

Conclusive DREAM validation using remote sensing methods has not yet been attained in the desert southwestern US, and three reasons for this are given. First, it is difficult to retrieve accurate dust optical property measurements over bright surfaces using passive satellite remote sensing systems. Second, it is difficult to retrieve AOT with sunphotometers during dust storms due to the windy nature of the dust events and the corresponding clouds. Third, there is a lack of vertical resolution (lidar) data. No single aerosol measurement method is sufficient, but rather a multi-sensor, integrated approach is necessary for DREAM evaluation in the desert southwestern US.

Given such a multi-sensor, integrated approach, DREAM strengths and shortcoming could be evaluated in the desert southwestern US, leading to an improved model of dust transport and thus dust storm prediction. Data from this model could then be used as an input to public health decision support systems, resulting in fewer incidences of dust-related respiratory diseases, asthma, allergies, eye infections and vehicle crashes. Once validated, DREAM data could also be used to help understand climate forcing and other impacts of dust on climate and environment.

## ACKNOWLEDGMENTS

Financial support for this work was provided by the NASA Earth Science Research, Education and Applications Solutions Network (REASoN) project funds (CA#NNS04AA19A). Also, the author would like to acknowledge Dr. Christina Hsu at NASA GSFC for providing the MODIS Deep Blue AOT data product.

## REFERENCES

1. Kirkland, T. N., and J. Fierer, "Coccidioidomycosis: A Reemerging Infectious Disease," *Emerging Infectious Diseases*, **3**, No. 2, 192-199, 1996.
2. Perez, C., S. Nickovic, G. Pejanovic, J.M. Baldasano and E. Ozsoy, "Interactive dust-radiation modeling: a step to improve weather forecasts," *J. Geophys. Res.* (in press), 2006b.
3. Remer, L. A., Y. J. Kaufman, D. Tanre, S. Mattoo, D. A. Chu, J. V. Martins, R-R. Li, C. Ichoku, R. C. Levy, R. G. Kleidman, T. F. Eck, E. Vermote, B. N. Holben, "The MODIS aerosol algorithm, products and validation," *J. Atmos. Sci.*, **62**, 947-973, 2005.

4. Dror, I., and N. S. Kopeika, "Statistical models for the desert aerosol size distributions and comparison to MODTRAN models," *SPIE*, **2375**, 61-71, 1995.
5. Bohren, C. F., and D. R. Huffman, *Absorption and Scattering of Light by Small Particles*, John Wiley & Sons, Inc., New York, 1998.
6. Wallace, J. M., and P. V. Hobbs, *Atmospheric Science, An Introductory Survey*, pp. 1-14, Academic Press, San Diego, 1977.
7. Colbeck, I., *Physical and Chemical Properties of Aerosols*, p. 148, Blackie Academic & Professional, an imprint of Thomson Science, UK, 1998.
8. Hudspeth, W., S. Nickovic, D. Yin, B. Chandy, B. Barbaris, A. Budge, T. Budge, S. Baros, K. Benedict, C. Bales, C. Catrall, S. Morain, G. Sanchez, W. Sprigg, and K. Thome, "PHAiRS - A Public Health Decision Support System: Initial Results," *Presentation to the 31st International Symposium on Remote Sensing of the Environment*, Russian Federation, St. Petersburg, 2005.
9. Nickovic, S., G. Kallos, A. Papadopoulos, O. Kakaliagou, "A model for prediction of desert dust cycle in the atmosphere," *Journal of Geophysical Research*, **106**, Issue D16, 18113-18130, 2001.
10. Yin, D., S. Nickovic, B. Barbaris, B. Chandy, W. A. Sprigg, "Modeling wind-blown desert dust in the southwestern United States for public health warning: A case study," *Atmospheric Environment*, **39**, No. 33, 6243-6254, 2005.
11. Thome, K., personal correspondence, February, 2006.
12. King, M. D., Y. J. Kaufman, W. P. Menzel, and D. Tanre, "Remote Sensing of Cloud, Aerosol, and Water Vapor Properties from the Moderate Resolution Imaging Spectrometer (MODIS)," *IEEE Trans. on Geoscience and Remote Sensing*, **30**, No. 1, 2-27, 1992.
13. Kaufman, Y. J., D. Tanre, "Algorithm for remote sensing of tropospheric aerosol from MODIS," MODIS ATBD for product ID: MOD04," 1-85, 1998.
14. Hsu, N.C., S. Tsay, M. D. King, and J. R. Herman, "Aerosol Properties Over Bright-Reflecting Source Regions," *IEEE Transactions on Geoscience and Remote Sensing*, **42**, No. 3, 557-569, 2004.
15. Chu, D. A., Y. J. Kaufman, C. Ichoku, L. A. Remer, D. Tanre, B. N. Holben, "Validation of MODIS aerosol optical depth retrieval over land," *Geophysical Research Letters*, **29**, No. 12, 1-4, 2002.
16. King, M. D., W. P. Menzel, Y. J. Kaufman, D. Tanre, B. C. Gao, S. Platnick, S. A. Ackerman, L. A. Remer, R. Pincus, and P. A. Hubanks, "Cloud and aerosol properties, precipitable water, and profiles of temperature and water vapor from MODIS," *IEEE Trans. Geosci. Remote Sensing*, **41**, 442-458, 2003.
17. Liou, K. *An Introduction to Atmospheric Radiation, International Geophysics Series, Vol. 26*, Ch. 7, Academic Press, Orlando, 1980.
18. Holben, B. N., T. F. Eck, I. Slutsker, D. Tanre, J. P. Buis, A. Setzer, E. Vermote, J. A. Reagan, Y. J. Kaufman, T. Nakajima, F. Lavenue, I. Jankowiak, and A. Smirnov, "AERONET - A Federated Instrument Network and Data Archive for Aerosol Characterization," *Remote Sensing of the Environment*, **66**, 1-16, 1998.
19. Dubovik, O., A. Smirnov, B. N. Holben, M. D. King, Y. J. Kaufman, T. F. Eck, and I. Slutsker, "Accuracy assessments of aerosol optical properties retrieved from Aerosol Robotic Network (AERONET) Sun and sky radiance measurements," *Journal of Geophysical Research*, **105**, No. D8, 9791-9806, 2000.
20. Perez, C., S. Nickovic, J. M. Baldasano, M. Sicard, F. Rocadenbosch, V. E. Cachorro, "A long Saharan dust event over the western Mediterranean: Lidar, sun photometer observations and regional dust modeling." (in press) *J. Geo. Res.*, 1-37, 2006.
21. Welton, E., K. Voss, H. Fordon, H. Maring, A. Smirnov, B. Holben, B. Schmid, J. Livingston, P. Russell, P. Durkee, P. Formenti, and M. Andreae, "Ground-based lidar measurements of aerosols during ACE-2: instrument description, results, and comparisons with other ground-based and airborne measurements," *Tellus*, **52B**, No. 2, 636-751, 2000.
22. Fernald, F. G., "Analysis of atmospheric lidar observations: some comments," *Appl. Optics*, **23**, 652-653, 1984.
23. Winker, D. M., J. Pelon, M. P. McCormick, "The CALIPSO mission: Spaceborne lidar for observation of aerosols and clouds," *SPIE*, 4893, 2003.